Mon. Not. R. Astron. Soc. **330,** 219–224 (2002)

Exploiting magnification bias in ultradeep submillimetre-wave surveys using ALMA

A. W. Blain[1,2]★

[1]*Institute of Astronomy, Madingley Road, Cambridge, CB3 0HA*
[2]*Astronomy Department, California Institute of Technology, Pasadena, CA 91125, USA*

Accepted 2001 October 18. Received 2001 October 17; in original form 2001 May 30

ABSTRACT

The surface density of populations of galaxies with steep/shallow source counts is increased/decreased by gravitational lensing magnification. These effects are usually called 'magnification bias' and 'depletion', respectively. However, if sources are demagnified by lensing, then the situation is reversed, and the detectable surface density of galaxies with a shallow source count, as expected at the faintest flux densities, is increased. In general, demagnified sources are difficult to detect and study: exquisite subarcsec angular resolution and surface brightness sensitivity are required, and emission from the lensing object must not dominate the image. These unusual conditions are expected to be satisfied for observations made of the dense swarm of demagnified images that could form very close to the line of sight through the centre of a rich cluster of galaxies using the forthcoming submillimetre-wave Atacama Large Millimeter Array (ALMA) interferometer. The demagnified images of most of the background galaxies lying within about 1 arcmin of a rich cluster of galaxies could be detected in a single 18-arcsec-diameter ALMA field centred on the cluster core, providing an effective increase in the ALMA field of view. This technique could allow a representative sample of faint, 10–100 μJy submillimetre galaxies to be detected several times more rapidly than in a blank field.

Key words: gravitational lensing – methods: observational – galaxies: clusters: general – cosmology: observations – infrared: galaxies – radio continuum: galaxies.

1 INTRODUCTION

Gravitational lensing magnification can have a significant effect on the observability of a population of galaxies, via the effect of magnification bias. Magnified sources that would otherwise be too faint for detection in a practical time can be found (Smail, Ivison & Blain 1997; Altieri et al. 1999; Pettini et al. 2000; Ellis et al. 2001), and otherwise unresolvable substructure within a source can be revealed (Franx et al. 1997). Here the effect of magnification bias in the innermost core regions of rich clusters of galaxies (Broadhurst, Taylor & Peacock 1995) is discussed, in the context of deep observations at very high angular resolution using the (sub)millimetre-wave Atacama Large Millimeter Array (ALMA) interferometer (Blain 1997, 2001; Wootten 2001).[1] ALMA will be extremely sensitive, but has a small field of view compared with optical and radio telescopes, and so large-area ALMA surveys are relatively challenging (Blain 2001). The radius of the ALMA field of view is set by the diffraction limit of a 12-m antenna. The full width at half-maximum (FWHM) diameter of the telescope beam ranges from about 8 arcsec at 850 GHz/350μm to about 1.2 arcmin at 90 GHz/3.3 mm.

Here, the de-magnification of lensed images of background galaxies in the core of a rich cluster of galaxies is discussed as a tool to enhance the efficiency of ALMA to probe the population of very faint submillimetre-wave galaxies, as compared with observations in a blank field.

2 MAGNIFICATION BIAS AND DEPLETION

When planning a survey, it is important to know how quickly a certain number of galaxies can be detected using a telescope. If the galaxies being studied are described by a differential source count, in which the surface density of galaxies that have intrinsic flux densities between S and $S + \mathrm{d}S$ is $N(S)$, then imposing a gravitational lensing magnification factor μ modifies the count to $N'(S) = N(S/\mu)/\mu^2$. In general, μ is a function of both the redshift and relative position on the sky of source and lens. If $N(S)$ can be described by a power law, $N(S) \propto S^{\alpha}$, then the bias factor $B = N'/N = \mu^{-(2+\alpha)}$ (Canizares 1981; Borgeest, von Linde & Refsdal

★E-mail: awb@astro.caltech.edu

[1] Extensive information about ALMA can be found at the website http://www.alma.nrao.edu

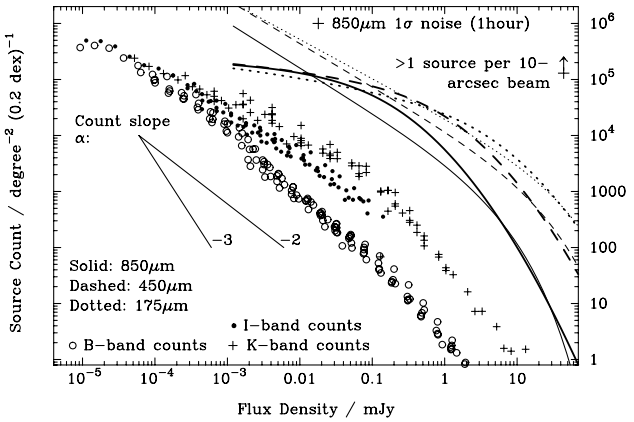

Figure 1. Differential source counts in the optical, near- and far-infrared and submillimetre wavebands. The *K*-, *I*- and *B*-band data come from the compilation of Metcalfe et al. (1996) and Maihara et al. (2001). Note that the faint slope of the *K*- and *B*-band counts are considerably different. The lines are associated with models for far-infrared and submillimetre-wave counts (thick: Blain et al. 1999b; thin: Blain et al. 1999c). These models agree with current observational results from SCUBA (Smail et al. 2001) at 850μm (from 1 to 10 mJy) and 450μm (from 10 to 20 mJy), and from *ISO* at 175μm from 180 to 500 mJy (Dole et al. 2001). The existing observational constraints are imposed at much brighter flux densities than those that ALMA will probe. The slope of the 850-μm counts fainter than about 1 mJy, and thus the magnification bias expected, is currently poorly defined, and awaits the results of SMA and ALMA observations. In the most pessimistic case, the slope will be similar to that of the faintest optical counts, and so the magnification bias will be small. In other models the slope of the faint submillimetre-wave counts could be very shallow leading to a strong bias.

1991; Schneider 1992). B takes a value greater than unity if the magnification bias is positive, and a value less than unity if the magnification bias is negative. If sources are magnified, that is, if $\mu > 1$, then the source count is increased if $\alpha < -2$, but reduced if $\alpha > -2$. If sources are demagnified, that is $\mu < 1$, then these conditions on α are reversed, and so a value of $\alpha > -2$ corresponds to a positive magnification bias.

In almost all the studies of high-redshift galaxy populations in which gravitational lensing is exploited, magnification rather than demagnification is utilized. The single existing exception is the use of the relative depletion of red galaxies, as compared with blue galaxies, behind rich clusters of galaxies to study the cluster potential in the absence of spectroscopic redshifts for all of the lensed background galaxies (Broadhurst et al. 1995; Gray et al. 2000; Dye et al. 2001). This differential depletion effect arises because of the different slopes of the faint counts from band to band: compare the slopes of the faint *B*- and *I*-band counts shown in Fig. 1.

3 THE DETECTION RATE OF GALAXIES

The importance of magnification bias for a galaxy survey depends on several factors.

First, there is a dependence on the slope of the source counts α, discussed above. The slope of the counts also determines the survey strategy that maximizes the detection rate of galaxies. In a fixed observing time, it is possible to trade-off area coverage and survey depth. Unless it is necessary to reach a certain depth in order to detect a specific class of objects, this trade-off favours a deep survey if $\alpha < -3$, and a wide survey if $\alpha > -3$. The appropriate trade-off in the submillimetre waveband, where count slopes can be very steep and change rapidly (Fig. 1), was discussed by Blain & Longair (1996).

Our present knowledge of submillimetre galaxy populations (Smail et al. 2001) is that the slope of the 850-μm counts is close to $\alpha = -3$ for flux densities between about 1 and 10 mJy (Fig. 1). This indicates that existing (sub)millimetre-wave galaxy surveys (Smail et al. 1997, 2001; Bertoldi et al. 2000; Scott et al. 2002) have been made at the most efficient depth: the detection rate is likely to be lower in both deeper and shallower surveys. It is likely, but not yet confirmed by observations, that the counts steepen at brighter flux densities. This could lead to a very large magnification bias at bright (>100 mJy) 850-μm flux densities (Blain 1997). The counts must become shallower, with $\alpha > -2$, at the faintest flux densities; otherwise, the sum of the flux density contributed by discrete sources would exceed the background radiation intensity measured by *COBE*-FIRAS (Fixsen et al. 1998).

Secondly, the ratio between the instantaneous field of view of a telescope and the size of the magnified field affects the significance of magnification bias. If the field of view of the telescope is very much larger than the magnified region – as is the case in the optical, radio, and X-ray wavebands, and soon in the mid-infrared waveband with the launch of *SIRTF* – then magnification bias is unlikely to provide a significant assistance to a survey. For example, even the optical WFPC-II camera on the *Hubble Space Telescope* (*HST*), with a 2-arcmin field of view that is small by current standards, can image almost all of the critical lensing region of a typical cluster of galaxies in a single pointing (for example, Smith et al. 2001). A single WFPC-II image of a cluster of galaxies can be used to probe simultaneously the low-magnification ($\mu \simeq 1$) regions well outside critical lines, the high-magnification ($\mu \gg 1$) regions close to the critical lines, and the demagnified ($\mu < 1$) region well within the critical lines close to the core of the cluster. This is even more true for the 3×3 arcmin field of view of the forthcoming *HST*-ACS camera. However, if the field of view is small compared with the strongly magnified area, then even a relatively modest magnification bias can have a significant effect. This is especially important if a telescope is only sufficiently sensitive to detect a handful of sources in a reasonable integration time, as is the case for existing submillimetre-wave observations (Smail et al. 2001).

Thirdly, the limit imposed to the maximum depth of a survey due to confusion noise can be significant. If the unmagnified population of galaxies is too faint to detect above this limit, then the exploitation of magnification bias is essential in order to make reliable detections. This is the case for the deepest existing submillimetre-wave surveys (Blain, Ivison & Smail 1998).

4 MAGNIFICATION BIAS AND ALMA

Although the most efficient detection rate of 850-μm galaxies is likely to be at a depth of 5 to 10 mJy, it is essential to obtain fainter counts, both to probe the properties of sub-L^* high-redshift galaxies, and to be sure of the relationship between the counts and the integrated intensity of background radiation. It is clear from Fig. 1 that models which provide an adequate description of existing data at mJy flux densities (Blain et al. 1999b,c) make quite different predictions for fainter counts, and so a measurement of very deep submillimetre-wave counts could reveal important new information about the evolution of high-redshift galaxies.

Because of source confusion, only interferometers with subarcsec resolution, that is, ALMA and the Submillimeter

Array (SMA; Ho 2000),[2] can make these observations. The importance of excellent resolution can be seen from the counts in Fig. 1. At an extreme depth of 1 μJy, the surface density of galaxies in the model which predicts the greatest count corresponds to only 1 source per 30 0.1-arcsec beams. This is a standard definition for a confused image, and a resolution limit of 0.1 arcsec is well within the capabilities of ALMA.

In a 1-h integration, within the 18-arcsec-diameter FWHM primary beam, the 1σ sensitivity of ALMA is 18 μJy at 345 GHz/870 μm (Wootten 2001). In a 100-h integration in a single field, about 20 detections would be expected at flux densities brighter than a 5σ threshold of 9 μJy. In the same area, a single detection would be expected at a 5σ threshold of 0.2 mJy, corresponding to a 0.2-h integration. Hence, many more galaxies (about 500) could be detected if ALMA were instead to map 100 different fields for 1 h each. From a comparison of these results, it is clear that a shallower, wider ALMA survey is expected to be more efficient at discovering faint submillimetre-wave galaxies. Because of the sensitivity of ALMA to CO line emission at very high redshifts (Blain et al. 2000), an ultradeep pencil-beam redshift survey would be a direct by-product.

Can gravitational lensing be exploited to assist ALMA to probe faint submillimetre-wave counts more rapidly? One route would be to exploit the high magnifications along critical lines in the image plane of a rich cluster of galaxies (Blain 2001) in order to detect the magnified images of very faint background galaxies. These would be intrinsically interesting sources, regardless of whether magnification bias increases or decreases their detection rate. The length of critical lines for a rich cluster at a moderate redshift is of the order of 5 arcmin, and so about 20 pointings with ALMA at 345 GHz would be required to map them. A similarly motivated approach would be to image moderate-redshift field galaxies in single deep ALMA pointings, especially those classes of galaxies with significant lensing cross sections, such as massive ellipticals and edge-on disc galaxies (see fig. 7 in Blain, Möller & Maller 1999a), in order to detect strongly lensed magnified images of faint background galaxies. Alternatively, it would be possible to exploit the very high angular resolution of ALMA to image the densely packed, demagnified counter-images of background galaxies that are expected to lie very close to the core of a cluster, well within the extent of the critical line structure, and also within the diameter of the ALMA primary beam. If the slope of the count of very faint background galaxies is flat, with $\alpha > -2$, then the bias factor B will be greater than unity.

The formal description of the lensing properties of the innermost regions of a cluster is relatively straightforward. Making the assumption of cylindrical symmetry, which is likely to be reasonable, the deflection angle of light θ_α at an impact parameter r depends on the mass enclosed $M(<r)$ as $\theta_\alpha \propto M(<r)/r$. If a spherical density profile with an index ξ, $\rho(r) \propto r^\xi$, is assumed, then $\theta_\alpha \propto r^{\xi+2}$. It is reasonable to assume a constant value of the index ξ, as we are concerned with only the very central regions of clusters. Using the lens equation to relate the angular diameter distances connecting the observer, lens and source, the magnification

$$\mu = \left|1 - \frac{D_{\rm LS}}{D_{\rm OS}}\,\theta_\alpha(\theta_{\rm I})\right|^{-1} \left|1 - (\xi+2)\frac{D_{\rm LS}}{D_{\rm OS}}\,\theta_\alpha(\theta_{\rm I})\right|^{-1}, \qquad (1)$$

[2] Information about SMA can be found at the website http://sma2.harvard.edu

where $\theta_{\rm I}$ is the angular position of the image. This can be re-expressed more simply in terms of the Einstein radius $\theta_{\rm E}$, as

$$\mu = \left|1 - \left(\frac{\theta_{\rm I}}{\theta_{\rm E}}\right)^{\xi+1}\right|^{-1} \left|1 - (\xi+2)\left(\frac{\theta_{\rm I}}{\theta_{\rm E}}\right)^{\xi+1}\right|^{-1} \qquad (2)$$

(Schneider, Ehlers & Falco 1992). The first and second terms yield the conditions for the formation of transverse and radial giant arc images respectively. The simplest form of the equation occurs for a singular isothermal sphere (SIS) with $\xi = -2$, in which case the second term vanishes; this is likely to be an extreme lower bound on the value of ξ. Note that the description breaks down if $\xi = -1$, which corresponds to the index for a Navarro–Frenk–White (NFW) density profile (Navarro, Frenk & White 1997), as derived from halo profiles extracted from *N*-body simulations. In this case, high-magnification radial-arc images are expected to dominate throughout the core of a cluster and almost no demagnified region is expected. The presence of dark and baryonic matter associated with a cD galaxy in the core of the cluster is sure to generate an index steeper than $\xi = -1$ in realistic cases, even if the dark-matter profile is described by an NFW profile. Alternative *N*-body simulations have indicated values of $\xi \simeq -1.4$ (Moore et al. 1998), while observations of X-ray gas profiles (for example Makino & Asano 1999) and *HST* images (for example Hammer et al. 1997) have been used to derive values of $\xi \simeq -1.4$ to -1.7 in the central regions of clusters. The magnification expected as a function of distance from the core of a circularly symmetric cluster is compared as a function of ξ in Fig. 2. An SIS produces the most significant demagnification.

In individual clusters, the magnification distribution is certain to be more complex, due to both the gravitational potential of the cluster member galaxies and the true aspherical, non-isothermal nature of the cluster dark-matter halo; however, in reasonable cases, with $\xi \sim -1.5$, strong de-magnification is always expected within a few arcsec of the core.

In order to make a coarse estimate of the maximum size of the effect, it is reasonable to assume an SIS radial density profile and $\theta_{\rm E} \simeq 40$ arcsec for a moderate-redshift rich cluster similar to Abell

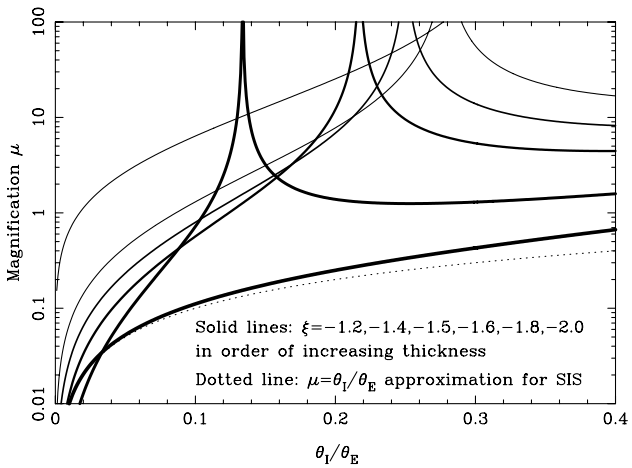

Figure 2. The magnification distribution (equation 2) expected as a function of angular radius $\theta_{\rm I}$, in units of the Einstein radius $\theta_{\rm E}$ for clusters with a range of different central density profile indices ξ; note that $\xi = -1$ and -2 for an NFW profile and SIS respectively. The high-magnification spikes are due to the formation of radial-arc images, which occur for $\xi > -2$. Within the radial-arc radius significant demagnifications ($\mu < 1$) are expected.

Table 1. Values of the magnification bias parameter $\bar{B}$ expected in the innermost region of a rich cluster with an Einstein radius $\theta_E = 40$ arcsec, for three different values of the power-law indices of the background galaxy count α, the inner radial density profile ξ, and the FWHM diameter of Gaussian primary beams θ_b. Values of $\theta_b = 36$, 18 and 9 arcsec correspond to the beams of the SMA at 850 μm, and of ALMA at 850 and 450μm respectively. The results in a simple approximation to the SIS magnification distribution, as marked by $\xi \simeq -2$, with $\bar{B} \propto (\theta_E/\theta_b)^{2+\alpha}$ are also listed.

θ_b/arcsec	α	ξ	$\bar{B}$	θ_b/arcsec	α	ξ	$\bar{B}$
36	−1.84	−2.0	1.04	36	−1.84	−1.6	0.76
36	−1.84	−1.4	0.64	36	−1.84	≃−2	1.16
36	−1.52	−2.0	1.24	36	−1.52	−1.6	0.49
36	−1.52	−1.4	0.30	36	−1.52	≃−2	1.63
36	−1.30	−2.0	1.53	36	−1.30	−1.6	0.42
36	−1.30	−1.4	0.20	36	−1.30	≃−2	2.13
18	−1.84	−2.0	1.24	18	−1.84	−1.6	0.85
18	−1.84	−1.4	0.73	18	−1.84	≃−2	1.30
18	−1.52	−2.0	2.03	18	−1.52	−1.6	0.75
18	−1.52	−1.4	0.47	18	−1.52	≃−2	2.27
18	−1.30	−2.0	3.00	18	−1.30	−1.6	0.85
18	−1.30	−1.4	0.42	18	−1.30	≃−2	3.46
9.0	−1.84	−2.0	1.42	9.0	−1.84	−1.6	1.06
9.0	−1.84	−1.4	0.93	9.0	−1.84	≃−2	1.45
9.0	−1.52	−2.0	3.01	9.0	−1.52	−1.6	1.48
9.0	−1.52	−1.4	0.92	9.0	−1.52	≃−2	3.17
9.0	−1.30	−2.0	5.25	9.0	−1.30	−1.6	2.18
9.0	−1.30	−1.4	1.01	9.0	−1.30	≃−2	5.62

2218. At small radii, $\theta_I \ll \theta_E$, $\mu \simeq \theta_I/\theta_E$ – see equation (2) and the dotted line in Fig. 2 – and so, as a function of radius θ, the bias factor $B = \mu^{-(2+\alpha)} = (\theta/\theta_E)^{-(2+\alpha)}$. When averaged over a top-hat beam of diameter θ_b, $\bar{B} \simeq 2^{3+\alpha}(\theta_E/\theta_b)^{2+\alpha}/(-\alpha)$, while for a Gaussian beam with FWHM diameter θ_b, $\bar{B} = (\theta_E/\theta_b)^{2+\alpha} \times (4 \ln 2)^{1+(\alpha/2)}\Gamma(-\alpha/2)$.

Values of the effective bias $\bar{B}$ calculated exactly using equation (2) for three different count slopes, $\alpha = -1.84$ (Blain et al. 1999c), -1.52 (Blain et al. 1999b) and -1.3, and for three different FWHM Gaussian beam sizes θ_b are listed in Table 1. Results are presented for three values of the density profile index ξ: an SIS model with $\xi = -2$, and two more realistic models with $\xi = -1.6$ and -1.4, which straddle the value $\xi = -1.5$ derived from *N*-body simulations by Moore et al. (1998). For the more realistic models the effective bias values are less than for the SIS case, but in most cases positive magnification bias is expected, at least in the innermost demagnified regions. Some of the bias values listed in Table 1 are less than unity, corresponding to a reduction in the surface density of images. This reduction is greatest for the largest beamsize, where the positive bias in the central demagnified region is counteracted by the negative bias in the surrounding region where $\mu > 1$, and for both less centrally concentrated clusters and steeper source counts. Within the innermost regions of all the cluster images, positive bias would still be expected in all cases.

It is possible, but not currently certain, that the ultradeep submillimetre-wave counts could have different slopes at different wavelengths. Hence, a differential magnification bias could be detected as a function of colour, a submillimetre-wave counterpart to the depletion signal detected in optical–near-infrared observations by Gray et al. (2000).

Prior to ALMA being commissioned, it will be interesting to search for this effect using the SMA. At 345 GHz, the best resolution of the SMA is expected to be 0.25 arcsec, and a 1σ sensitivity of 1 mJy is expected in an 8-h integration. The resolution is thus probably too coarse, and the sensitivity insufficiently great to exploit the demagnification bias effect to the full.

Although the magnification bias can increase the surface density of detectable galaxies in the innermost parts of clusters, this increase corresponds to a reduction in the fraction of the background radiation intensity that is resolved in detected galaxies. In order to detect the greatest possible proportion of the submillimetre-wave background radiation intensity, ALMA observations of the most strongly magnified regions of clusters of galaxies are still required.

4.1 Potential caveats

'Demagnification bias' could make observations of extremely faint counts of galaxies significantly easier using ALMA, if the slope of the faint counts is shallow, $\alpha \gtrsim -1.5$, and the density profile of the cluster is centrally peaked, $\xi \lesssim -1.5$. However, it can only be exploited if both the angular resolution of the resulting images is sufficient to allow adjacent lensed images to be resolved, and the confusion limit is sufficiently deep. The physical extent of the lensed background galaxies must also be small enough to avoid them overlapping on the sky, and there must be no strong emission or absorption from the lensing cluster to mask the demagnified sources.

4.1.1 Resolution, confusion and source size

Several tens of resolution elements per source within the primary beam are required to satisfy both the confusion and resolution requirements. This relates to a resolution of the order of 0.1 arcsec, which will easily be achieved using ALMA at a wavelength of 850 μm on even a relatively short 2-km baseline. At the maximum planned 10-km baseline, the resolution at 850 and 450 μm is considerably better; 0.02 and 0.01 arcsec, respectively. The source sizes should also be sufficiently small. There is evidence for large haloes of cold gas around the most luminous high-redshift dust-enshrouded galaxies (Papadopoulos et al. 2001), but other sources are known to be smaller than a few arcsec in size (Frayer et al. 1998, 1999, 2000; Downes et al. 1999; Lutz et al. 2001). They will also be reduced in extent by demagnification.

4.1.2 Contamination from cluster emission

A great advantage of the *K*-correction in the submillimetre waveband is that high-redshift galaxies are as easy to detect as their low-redshift counterparts (Blain & Longair 1993). This is verified by the lack of a significant fraction of low-redshift galaxies detected in SCUBA surveys (Smail et al. 2001), with the exception of two cD galaxies in the centres of the target clusters containing powerful cooling flows (Edge et al. 1999).

Submillimetre-wave emission from the interstellar medium (ISM) in cD galaxies is intrinsically interesting, as it could reveal the fate of gas that cools from the X-ray emitting intracluster medium. However, it could also mask the demagnified images of background galaxies in an extremely deep ALMA observation. Even magnified radial-arc images can be masked by starlight from cD galaxies in optical *HST* images (Smith et al. 2001).

It is likely that any contaminating emission from the cD galaxy ISM could be subtracted reliably from the ALMA images. ALMA has the sensitivity to resolve this emission in several different CO transitions. The cD emission is also likely to be spread over an area of at least several square arcsec, and so should have a reduced

surface brightness as compared with the images of background galaxies. In addition, the continuum radiation from the background galaxies will undergo molecular line absorption at the redshift of the cD galaxy, and so by searching for these narrow absorption lines it should be possible to further discriminate between emission from background images and the cD galaxy. Absorption by gas within the cluster and cD galaxy is not likely to be important away from the frequencies of these discrete absorption lines.

4.2 Determining the central cluster potential and the geometry of the Universe

Based on the observed positions of many sets of multiple images of background galaxies detected using ALMA, a significant fraction of which will certainly be identified correctly, with redshifts determined serendipitously from the detection of CO lines (Blain et al. 2000; Blain 2001), it should be possible to accurately reconstruct the gravitational potential very close to the cluster core, and so reveal the density profile of both visible and dark matter. This is impossible using optical observations, as starlight from the cD galaxy masks the lensed images. The detection of any magnified radial-arc images within 10–20 arcsec of the cluster core (see Fig. 2) would also provide useful constraints on the gradient of the local potential.

The magnified counter-images to the demagnified images detected in the innermost regions of the cluster are expected to lie close to critical lines. Knowledge of their positions, especially of those sets of multiple images confirmed using CO redshifts, can be used to construct exact mass models of the inner few arcmin of the lensing cluster. In addition, several sets of multiple images with redshifts could be used to investigate the geometry of the Universe by finding the relative geometrical distances between the observer, cluster and source; compare with the triplet method of Gautret, Fort & Mellier (2000) for weak lensing.

The time required to complete such a multiple imaging survey should be comparable to the time required to image the demagnified central region of the cluster. The magnified counter-images are expected to lie close to critical lines, and so could be detected in a series of about 20 ALMA images forming a ring around the centre of a cluster. These images would be significantly brighter than the central demagnified images, and so a shorter integration time per field would be required. Over many years, it would be desirable to build up multiwavelength ALMA images of the entire central regions of clusters; however, maps of both the innermost core and the critical lines, generating a bullseye image, with a central ultradeep field in the core, surrounded by an annulus of shallower observations tracing the critical lines several tens of arcsec away, are the most urgent requirements.

This type of survey will not provide a fully representative sample of the distant Universe, as it is necessarily limited to 1-arcmin-diameter pencil beams passing through the cores of at most several hundred rich clusters at intermediate redshifts. However, it will provide an increased efficiency for the determination of the very faintest submillimetre-wave counts.

5 CONCLUSIONS

At the depths suitable for the detection of a number of galaxies within the primary beam of ALMA, the differential submillimetre-wave source counts, $N \propto S^{\alpha}$ are likely to be rather flat, with $\alpha \gtrsim -1.8$. In the significantly demagnified regions within about 10 arcsec of the cores of rich clusters of galaxies, this corresponds to an increase in the surface density of faint sub-100 μJy galaxies. Ultradeep ALMA images of the innermost regions of cluster cores could thus speed the detection of the population of normal, L^* high-redshift galaxies, if clusters have a central density profile index $\xi \lesssim -1.5$ and the faint count slope $\alpha \gtrsim -1.5$. An ultradeep pencil-beam redshift survey would be provided as a by-product, from the simultaneous detection of CO emission and absorption lines in the spectra of the detected galaxies. By detecting several sets of magnified counter-images to these sources, which would lie at radii of order 1 arcmin from the cluster core, it should be possible to provide accurate measures of both the central cluster potential and the geometry of the Universe.

ACKNOWLEDGMENTS

Thanks to Ole Möller, Priya Natarajan, Kate Quirk and an anonymous referee for valuable comments on the manuscript. AWB acknowledges generous support from the Raymond and Beverly Sackler Foundation as part of the Deep Sky Initiative programme at the IoA.

REFERENCES

Altieri B. et al., 1999, A&A, 343, L65
Bertoldi F. et al., 2000, A&A, 360, 92
Blain A. W., 1997, MNRAS, 290, 553
Blain A. W., 2001, in Wootten A., ed., ASP Conf. Ser. Vol. 235, Science with ALMA. Astron. Soc. Pac, San Francisco in press (astro-ph/9911449)
Blain A. W., Longair M. S., 1993, MNRAS, 264, 509
Blain A. W., Longair M. S., 1996, MNRAS, 279, 847
Blain A. W., Ivison R. J., Smail I., 1998, MNRAS, 296, L29
Blain A. W., Möller O., Maller A. H., 1999a, MNRAS, 303, 423
Blain A. W., Smail I., Ivison R. J., Kneib J.-P., 1999b, MNRAS, 302, 632
Blain A. W., Jameson A., Smail I., Longair M. S., Kneib J.-P., Ivison R. J., 1999c, MNRAS, 309, 715
Blain A. W., Frayer D. T., Bock J. J., Scoville N. Z., 2000, MNRAS, 313, 559
Borgeest U., von Linde J., Refsdal S., 1991, A&A, 251, L35
Broadhurst T. J., Taylor A. N., Peacock J. A., 1995, ApJ, 438, 49
Canizares C. R., 1981, Nat, 291, 620
Dole H. et al., 2001, A&A, 372, 364
Downes D. et al., 1999, A&A, 347, 809
Dye S., Taylor A. N., Thommes E. M., Meisenheimer K., Wolf C., Peacock J. A., 2001, MNRAS, 321, 685
Edge A. C., Ivison R. J., Smail I., Blain A. W., Kneib J.-P., 1999, MNRAS, 306, 599
Ellis R. S., Santos M., Kneib J.-P., Kuijken K., 2001, ApJ, 560, L119
Fixsen D. J., Dwek E., Mather J. C., Bennett C. L., Shafer R. A., 1998, ApJ, 508, 123
Franx M., Illingworth G. D., Kelson D. D., van Dokkum P. G., Tran K.-V., 1997, ApJ, 486, L75
Frayer D. T., Ivison R. J., Scoville N. Z., Yun M., Evans A. S., Smail I., Blain A. W., Kneib J.-P., 1998, ApJ, 506, L7
Frayer D. T. et al., 1999, ApJ, 514, L13
Frayer D. T., Smail I., Ivison R. J., Scoville N. Z., 2000, AJ, 120, 1668
Gautret L., Fort B., Mellier Y., 2000, A&A, 353, 10
Gray M. E., Ellis R. S., Refregier A., Bézecourt J., McMahon R. G., Beckett M. G., Mackay C. D., Hoenig M. D., 2000, MNRAS, 318, 573
Hammer F., Gioia I. M., Shaya E. J., Teyssandier P., Le Fevre O., Luppino G. A., 1997, ApJ, 491, 477
Ho P. T. P., 2000, in Mangum J., ed., ASP Conf. Ser. Vol. 217, Imaging at Radio through Submillimeter Wavelengths. Astron. Soc. Pac, San Francisco, p. 26
Lutz D. et al., 2001, A&A, 378, 70

Maihara T. et al., 2001, PASP, 53, 25
Makino N., Asano K., 1999, ApJ, 512, 9
Metcalfe N., Shanks T., Campos A., Fong R., Gardner J. P., 1996, Nat, 294, 147
Moore B., Governato F., Quinn T., Stadel J., Lake G., 1998, ApJ, 499, L5
Navarro J. F., Frenk C. S., White S. D. M., 1997, ApJ, 462, 563
Papadopoulos P., Ivison R., Carilli C., Lewis G., 2001, Nat, 409, 58
Pettini M., Steidel C., Adelberger K. Ł., Dickinson M., Giavalisco M., 2000, ApJ, 528, 96
Schneider P., 1992, A&A, 254, 14
Schneider P., Ehlers J., Falco E. E., 1992, Gravitational lenses. Springer, Berlin, p. 230
Scott S. et al., 2002, MNRAS, submitted (astro-ph/0107446)
Smail I., Ivison R. J., Blain A. W., 1997, ApJ, 490, L5
Smail I., Ivison R. J., Blain A. W., Kneib J.-P., 2001, MNRAS, submitted
Smith G. P., Kneib J.-P., Eberling H., Czoske O., Smail I., 2001, ApJ, 552, 493
Wootten A., ed., 2001, ASP Conf. Ser. Vol. 235, Science with ALMA. Astron. Soc. Pac, San Francisco, in press

This paper has been typeset from a TEX/LATEX file prepared by the author.